Supplemental material

Sirka et al., https://doi.org/10.1083/jcb.201802144

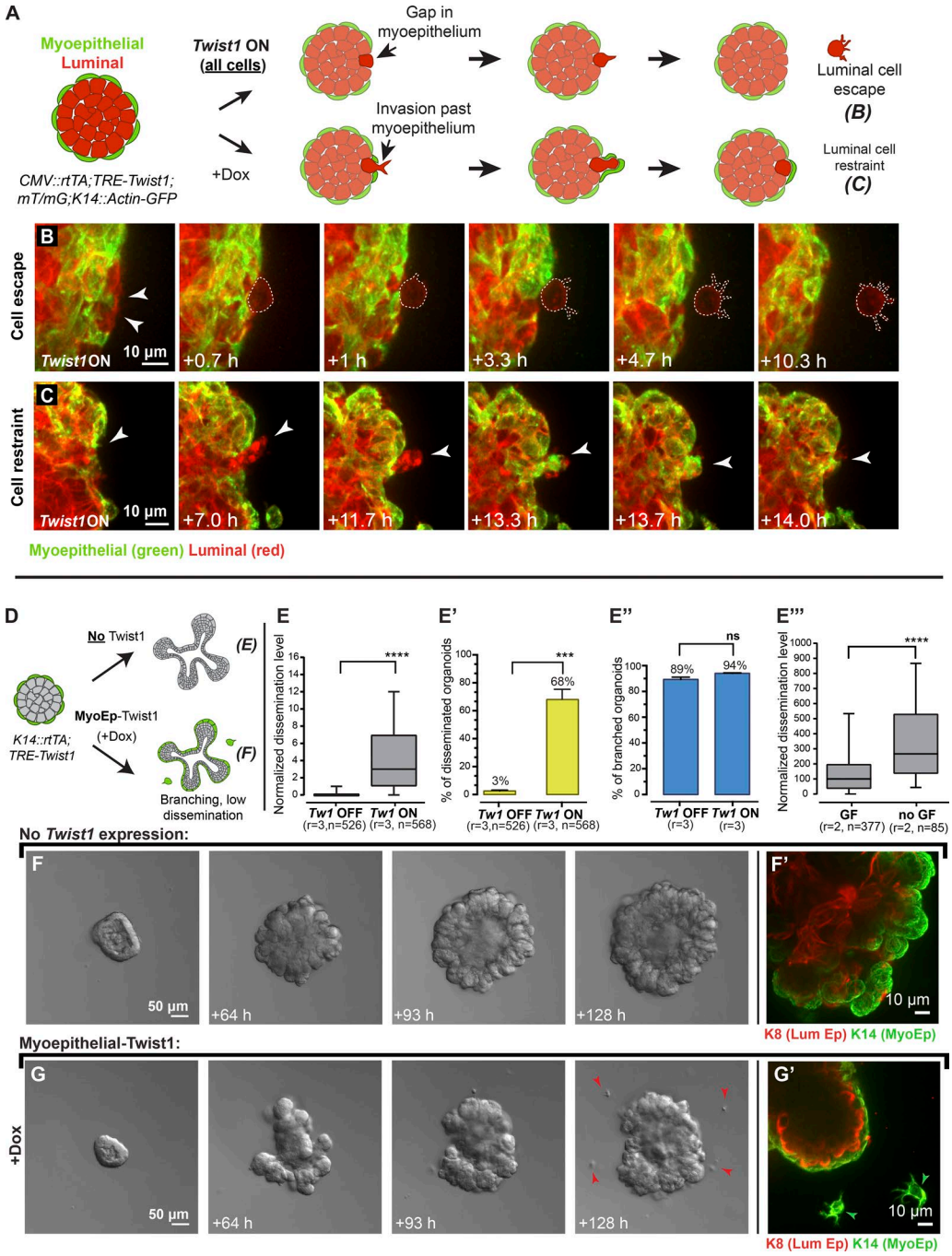

Figure S1. **The myoepithelium appears to restrain protruding Twist1⁺ luminal cells in the Ubiquitous-Twist1 model, and *Twist1* expression results in cell-autonomous dissemination in the Myoepithelial-Twist1 model. (A)** Fluorescent reporters were used to monitor real-time interactions between myoepithelial cells and luminal cells in *CMV::rtTA;TRE-Twist1;mT/mG;K14::Actin-GFP* organoids with constitutive *Twist1* expression. **(B)** Luminal cells (white dotted lines) were observed to disseminate through gaps in the myoepithelium. **(C)** Luminal cells that protruded past the myoepithelium (arrowheads) could also be restrained by myoepithelial cells. **(D)** Myoepithelial-specific *Twist1* expression was induced with doxycycline (Dox) in organoids isolated from *K14::rtTA;TRE-Twist1* mice. **(E and E')** Dissemination occurred in 68% of organoids upon addition of doxycycline. **(E'')** Organoids branched at similar rates with and without *Twist1* expression. **(E''')** Dissemination levels were increased in the absence of FGF2 (GF). **(F and F')** Control organoids maintained normal tissue architecture. **(G and G')** In contrast, myoepithelial *Twist1* expression resulted in dissemination (red arrowheads) of K14⁺ cells (green arrowheads). K8⁺ cells remained within the organoid. n, total number of organoids; r, number of biological replicates. Data in E and E''' were analyzed by two-tailed nonparametric Mann–Whitney–Wilcoxon test: ****, $P < 0.0001$. Data are presented as box plots, with error bars representing the 5th to 95th percentile. Data in E' and E'' was analyzed by two-tailed unpaired *t* test with equal SD; ***, $P < 0.001$. Error bars represent mean ± SEM.

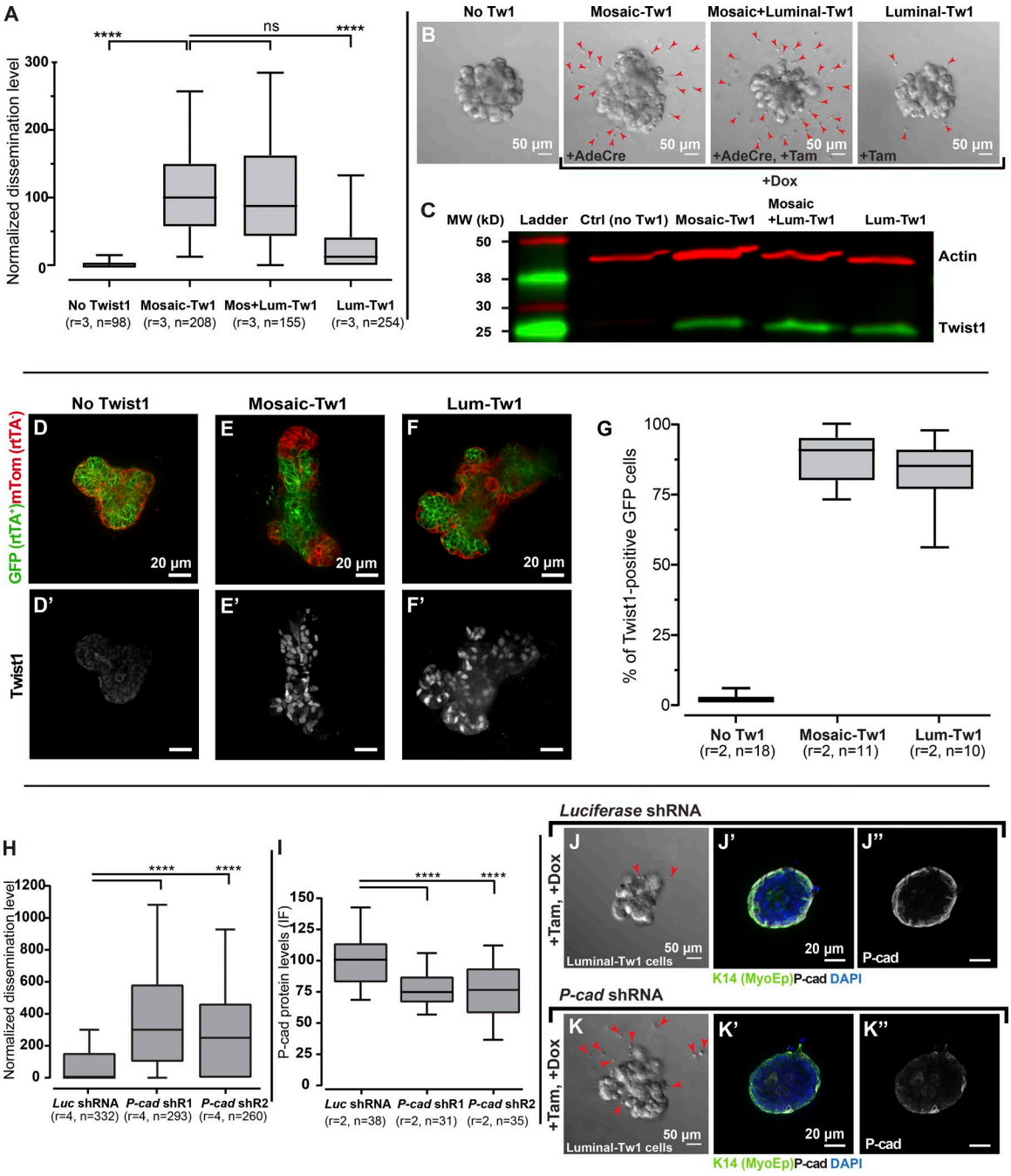

Figure S2. **Luminal-specific *Twist1* expression rarely results in dissemination despite abundant Twist1⁺ cells and is increased by *P-cadherin* knockdown. (A)** Dissemination was quantified in *K8::Cre-ER;R26::LSL-rtTA;TRE-Twist1* organoids with no *Twist1* expression (no Twist1) versus those with *Twist1* expression regulated by Adeno-Cre–(Mosaic-Tw1), by both Adeno-Cre and a tamoxifen (Tam)-inducible Cre-ER(Mosaic+Lum-Tw1), and by tamoxifen-inducible Cre-ER alone (Lum-Tw1). **(B)** Representative images of the conditions from A. Arrowheads indicate disseminated cells. **(C)** Western blot of the conditions from A showing that Twist1 protein levels are similar across methods of *Twist1* induction and not affected by tamoxifen addition. **(D–G)** Nuclear Twist1 was observed in a majority of recombined GFP-positive cells in Mosaic-Twist1 and Luminal-Twist1 models. **(H–K″)** Organoids isolated from *K8::Cre-ER;R26::LSL-rtTA;TRE-Twist1* mice were treated with lentiviral shRNA against *Luciferase* (control) and two different hairpins targeting *P-cadherin* (*P-cad*; myoepithelial adhesion gene). Organoids were treated with tamoxifen to induce *rtTA* expression and cultured in doxycycline (Dox) to induce *Twist1* expression in the luminal cell compartment. Organoids were divided into control and P-cadherin knockdown treatment groups. The number of disseminated cells per organoid was significantly higher in P-cadherin knockdown organoids compared with the control (two- to threefold difference) across four biological replicates (H, J, and K). Red and white arrowheads indicate disseminated cells. P-cadherin protein levels quantified from IF images confirmed a decrease in P-cadherin protein in P-cadherin knockdown organoids (I). IF demonstrated retention of K14 and reduction in P-cadherin in P-cadherin knockdown organoids (K′ and K″). n, total number of organoids; r, number of biological replicates. Data were analyzed by two-tailed nonparametric Kruskal–Wallis multiple comparisons test: ****, $P < 0.0001$. Data are presented as box plots, with error bars representing the 5th to 95th percentile.

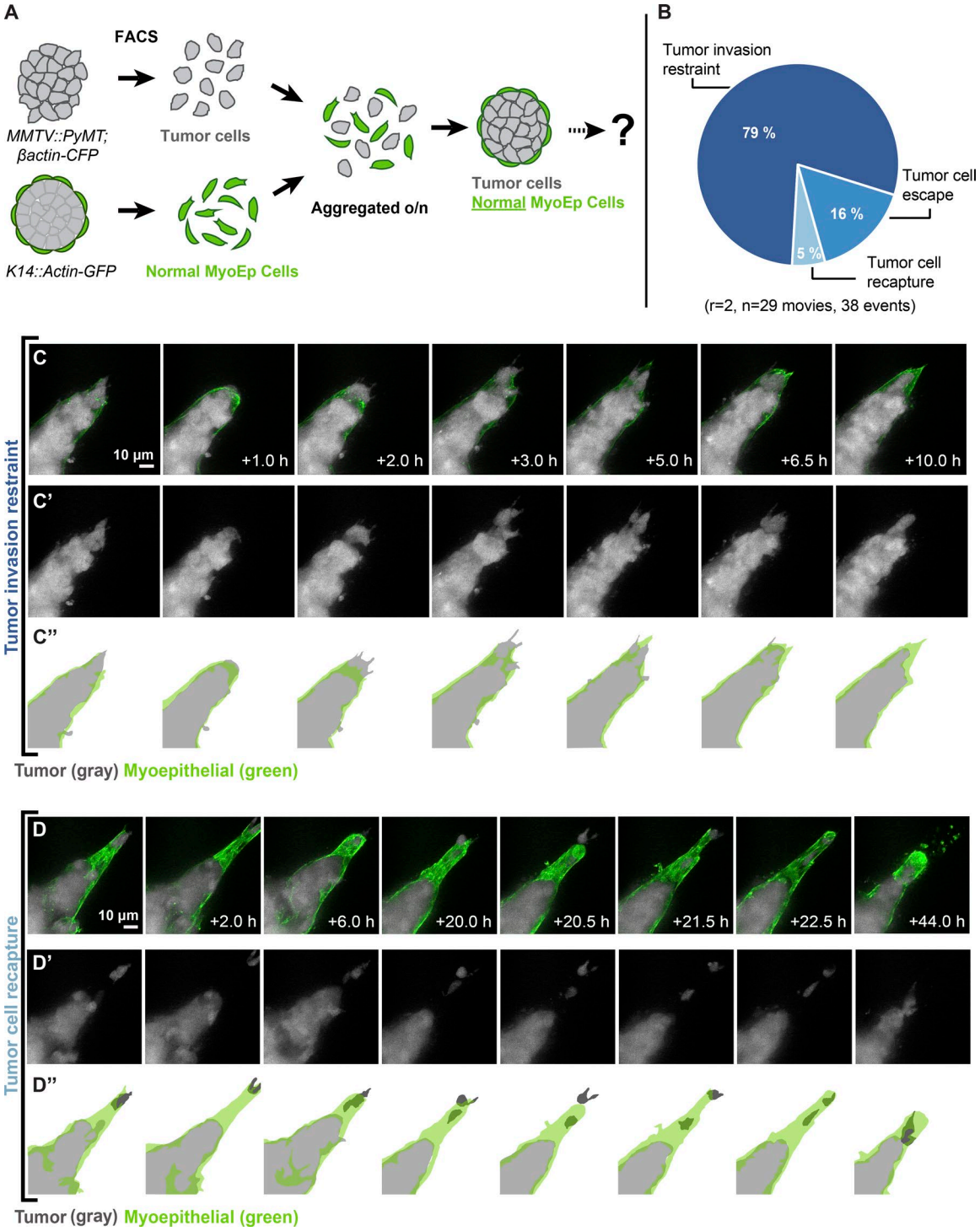

Figure S3. **Normal myoepithelial cells suppress invasion and dissemination of PyMT tumor cells. (A)** Tumor cells (CFP$^+$; gray) were isolated from *MMTV::PyMT;βactin-CFP* mice, and normal myoepithelial cells (GFP$^+$; green) were isolated from *mT/mG;K14::Actin-GFP* mice via FACS. Tumor cells were aggregated with normal myoepithelial cells at different ratios to form clusters, and aggregated clusters were cultured in 3D collagen I. **(B)** Tumor cell restraint, recapture, and dissemination quantified from real-time confocal videos across multiple replicates. **(C–C'')** Myoepithelial cells appeared to suppress invasion of tumor cells by containing the invasive front and reestablishing a continuous myoepithelial layer. **(D–D'')** Myoepithelial cells were also observed to extend into the collagen and capture disseminated tumor cells. n, total number of videos analyzed; r, number of biological replicates. Myoepithelial cells in time-lapse videos are pseudocolored in green throughout the figure.

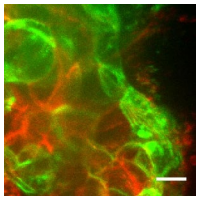

Video 1. **Luminal cell dissemination past normal myoepithelium.** 3D confocal time-lapse video portrays a rare event of Twist1⁺ luminal cell (red) disseminating through the Twist1⁻ myoepithelium (green) in a *K8::Cre-ER;R26::LSL-rtTA;TRE-Twist1;mT/mG* organoid (corresponds with Fig. 2 B). Frames were collected every 20 min for 17 h using a Solamere Technology Group spinning-disk confocal microscope with a 40×LD-LCI C-Apochromat oil lens. Video displayed at seven frames/s. Bar, 10 µm. Myoepithelial cells in the time-lapse video are pseudocolored in green.

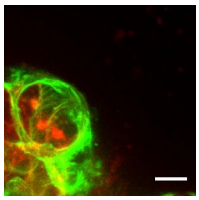

Video 2. **The myoepithelium dynamically restrains protruding Twist1⁺ luminal cells.** Representative 3D confocal time-lapse video of Twist1⁺ luminal cells (red) protruding past the Twist1⁻ myoepithelium (green) in a *K8::Cre-ER;R26::LSL-rtTA;TRE-Twist1;mT/mG* organoid. Adjacent myoepithelial cells migrated over and contained luminal cells (corresponds with Fig. 2 C). Frames were collected every 20 min for 12 h using a Solamere Technology Group spinning-disk confocal microscope with a 40×LD-LCI C-Apochromat oil lens. Video displayed at seven frames/s. Bar, 10 µm. Myoepithelial cells in the time-lapse video are pseudocolored in green.

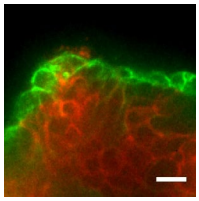

Video 3. **The myoepithelium contains protruding Twist1⁺ luminal cells.** An additional representative 3D confocal time-lapse video of Twist1⁺ luminal cells (red) protruding past the Twist1⁻ myoepithelium (green) in a *K8::Cre-ER;R26::LSL-rtTA;TRE-Twist1;mT/mG* organoid. Luminal cells that protruded past the myoepithelium were restrained by myoepithelial cells. Frames were collected every 20 min for 12 h using a Solamere Technology Group spinning-disk confocal microscope with a 40×LD-LCI C-Apochromat oil lens. Video displayed at seven frames/s. Bar, 10 µm. Myoepithelial cells in the time-lapse video are pseudocolored in green.

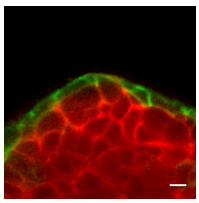

Video 4. **The myoepithelium restrains from escape a protruding Twist1⁺ luminal cell.** A 3D confocal time-lapse video of a Twist1⁺ luminal cell (red) protruding past the Twist1⁻ myoepithelium (green) in a *K8::Cre-ER;R26::LSL-rtTA;TRE-Twist1;mT/mG* organoid and being restrained from escape. Frames were collected every 20 min for 12 h using a Solamere Technology Group spinning-disk confocal microscope with a 40×LD-LCI C-Apochromat oil lens. Video displayed at seven frames/s. Bar, 10 µm. Myoepithelial cells in the time-lapse video are pseudocolored in green.

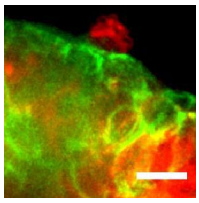

Video 5. **The myoepithelium covers and contains a protruding Twist1⁺ luminal cells.** An additional 3D confocal time-lapse video of a Twist1⁺ luminal cell (red) protruding past the Twist1⁻ myoepithelium (green) in a *K8::Cre-ER;R26::LSL-rtTA;TRE-Twist1;mT/mG* organoid and being contained by adjacent myoepithelial cells. Frames were collected every 20 min for 12 h using a Solamere Technology Group spinning-disk confocal microscope with a 40×LD-LCI C-Apochromat oil lens. Video displayed at seven frames/s. Bar, 10 µm. Myoepithelial cells in the time-lapse video are pseudocolored in green.

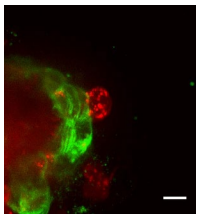

Video 6. **Luminal cell dissemination past *SMA*-depleted myoepithelium.** Organoids isolated from *K8::Cre-ER;R26::LSL-rtTA;TRE-Twist1;mT/mG* mice infected with lentiviral shRNA against *SMA*. Representative 3D confocal time-lapse video of Twist1⁺ luminal cells (red) escaping through SMA⁻ myoepithelium (green; corresponds with Fig. 4 F). Frames were collected every 20 min for 11 h using a Solamere Technology Group spinning-disk confocal microscope with a 40×LD-LCI C-Apochromat oil lens. Video displayed at seven frames/s. Bar, 10 µm. Myoepithelial cells in the time-lapse video are pseudocolored in green.

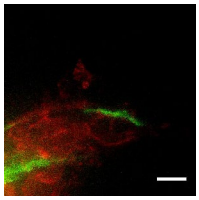

Video 7. **Normal myoepithelial cells limit invasion of basal tumor cells.** Tumor cells isolated from *C3-1-Tag;mT/mG* mice and normal myoepithelial cells isolated from *K14::Actin-GFP* mice were aggregated at different ratios to form clusters, followed by culturing aggregated clusters in 3D collagen I. 3D confocal time-lapse video portrays myoepithelial cells (green) restraining invasion of tumor cells (red) past the myoepithelial layer and reestablishing a continuous myoepithelial layer (corresponds with Fig. 5 D). Frames were collected every 30 min for 30 h using a Solamere Technology Group spinning-disk confocal microscope with a 40×LD-LCI C-Apochromat oil lens. Video displayed at seven frames/s. Bar, 10 µm. Myoepithelial cells in the time-lapse video are pseudocolored in green.

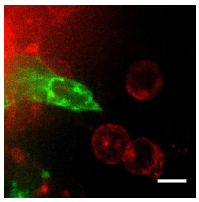

Video 8. **Normal myoepithelial cells recaptures disseminated basal tumor cells.** Tumor cells isolated from *C3-1-Tag;mT/mG* mice and normal myoepithelial cells isolated from *K14::Actin-GFP* mice were aggregated at different ratios to form clusters, followed by culturing aggregated clusters in 3D collagen I. 3D confocal time-lapse video portrays myoepithelial cells (green) reaching into collagen I and capturing disseminated tumor cells (red; corresponds with Fig. 5 E). Frames were collected every 30 min for 36 h using a Solamere Technology Group spinning-disk confocal microscope with a 40×LD-LCI C-Apochromat oil lens. Video displayed at 7 frames/s. Bar, 10 µm. Myoepithelial cells in the time-lapse video are pseudocolored in green.